JOURNAL OF MATERIALS SCIENCE 31 (1996) 5891–5896

Debinding and sintering defects from particle orientation in ceramic injection moulding

T. ZHANG*, S. BLACKBURN**, J. BRIDGWATER‡
IRC in Materials for High Performance Applications, The University of Birmingham, Edgbaston, Birmingham, B15 2TT, UK

The causes of the defects in injection-moulded ceramic bars during debinding and sintering were investigated using density and shrinkage measurements in combination with macroscopic observation. Differential shrinkage during sintering is the main cause of post-debinding defects. Particle shape, mould geometry and gate position have a large effect on this differential shrinkage, while the volumetric shrinkage is almost constant and the influences of moulding conditions are relatively small. Particles with plate-like morphology orientate during moulding and contribute markedly to defect formation during debinding and sintering.

1. Introduction

Injection moulding offers advantages in the economic production of complex-shaped parts from high-performance engineering materials [1, 2]. The main limitation is the control of defects and these can arise in any of the processing stages. The most significant defects which occur during injection moulding are voids and cracks. A computer modelling method to predict voids has been developed to reduce defect formation at this stage [3]; modulated pressure moulding and heated sprue moulding have been used to diminish void formation [4, 5]. The causes of defects during debinding and sintering are far more complicated and difficult to isolate. It is believed that the main factor is the binder extraction rate and thus great efforts have been made in controlling this rate [6–8]. However, it has also been observed that the defects which develop during debinding and sintering may originate from the injection stage. The moulded components may have a heterogeneous structure which will produce anisotropic properties with, for example, the thermal expansion varying with position and direction [9, 10]. There are several potential causes of this anisotropy.

1. Binder and powder segregation leading to non-uniform density distribution.
2. Relaxation of residual stress.
3. Binder orientation.
4. Particle orientation.

The first will cause positional property variation within the sample and is easy to distinguish by density or ashing (loss on ignition) measurements. The second can be expected to be small in the moulding of large cross-sections as stresses can relax during the lengthy cooling times in the mould. Residual stress measurements on an 11 mm thick injection-moulded plate have shown that they are much smaller than predicted and that component relaxation continued after removal from the mould [11, 12]. Binder and particle orientation have a significant effect on the anisotropy of the various component properties. Allan and Bevis [13] showed that, due to the orientation of polymer molecules, the differential shrinkage during relaxation in injection-moulded polymers could be significant, because the orientation of the molecules was not always parallel to the injection direction. Particle orientation has been studied in conventional ceramic processing by Cox and Williamson [14]. They show that when ball clay is cast or extruded, large differential shrinkages occurred during drying and firing. Particle orientation during tape casting [15] and hot-pressing [16] has also been investigated. However, because the test samples used were small (less than 3 mm thick), no defect development was observed. Previous research work has shown that during injection moulding, non-spherical particles will orientate and the orientation varies with position in the mould component [17].

This work explores the causes of defects which develop during debinding and sintering, considering the significance of injection processing and powder properties.

2. Experimental procedure

2.1. Materials and moulding conditions

Two grades of α-alumina were used; Baco RA107LS (Alcan Chemicals Ltd, UK) with a mean particle size of 0.5 μm and F1500 (Universal Ceramic Materials Ltd, UK) with a mean particle size of 2.9 μm

* *Present address*: School of Engineering Systems and Design, South Bank University, London, SE1 0AA, UK.
** and School of Chemical Engineering, The University of Birmingham
‡ *Present address*: Department of Chemical Engineering, University of Cambridge, Pembroke Street, Cambridge, CB2 3RA, UK.

0022–2461

(measured by X-ray photosedimentometry). The two powders had different morphologies, the RA107LS being tabular or plate-like and the F1500 more spherical but not well rounded, i.e. angular. The binders used were paraffin wax (PW, Shell Industrial Chemicals, UK) grade 130/135 FR, ethylene vinylacetate copolymer (EVA, Du Pont, UK) Elvax 140W, with di-*n*-butyl phthalate (DBP, BDH Chemicals, UK) and stearic acid (SA, BDH Chemicals, UK) as plasticizer and lubricant, respectively. The compositions of the mixes are shown in Table I, the volumetric concentrations being calculated from the densities of powders and binders.

Mixing was carried out in a Z-blade mixer (Werner and Pfleiderer, Stuttgart, FRG). Each batch was mixed for 1 h with a water circulation temperature (Grossenbacher Apparatebau AG., Switzerland) of 90 °C. An Arburg 250-75-270D (Arburg Maschinenfabrik Hehl and Soehne GmbH Co KG, Lossburg, FRG) injection-moulding machine was used to mould three types of samples at 20, 40 and 60 MPa and two speeds. The barrel was heated in four zones, set at 100–110–120–120 °C from the feed port to the nozzle. The mould temperature was held at 20 °C using circulating water (Grossenbacher Apparatebau AG., Switzerland). Fig. 1 shows (a) a bar of type A, size 15 mm × 20 mm × 65 mm, end gated, and (b) a bar of type B which was sectioned, so that bar samples with different gates were obtained, one end gated and the other centre gated. The dimensions were 6 mm × 8 mm × 60 mm.

2.2. Debinding and sintering

Debinding was carried out for all full bars of types A and B in air with the heating rate cycles given in Table II. In order to examine the internal structure of the mouldings, sections were cut from bars of type A as shown in Fig. 2 using a diamond saw. A powder bed of F1500 alumina powder was used to support all samples during debinding.

A number of samples were also annealed before debinding using a hot-pressing device specifically designed for the purpose. Each moulded bar was covered with a nylon bag and placed in a cylinder filled with hydraulic oil. The temperature was maintained at 120 °C for a soak time of 30 min at a pressure of 9 MPa. The sample was allowed to cool down in the annealer. The bars of type A annealed in the hydraulic device were sectioned to give samples of 5 mm × 5 mm × 45 mm (Fig. 2) and annealed again in an oven at 120 °C for 24 h.

TABLE I Moulding paste formulations

Materials	RA107LS		F1500	
	(wt %)	(vol %)	(wt %)	(vol %)
α-alumina	88.79	65.0	86.48	60.0
EVA	3.75	11.5	4.53	13.2
PW	3.75	11.9	4.53	13.6
SA	1.85	6.3	2.23	7.2
DBP	1.85	5.3	2.23	6.0

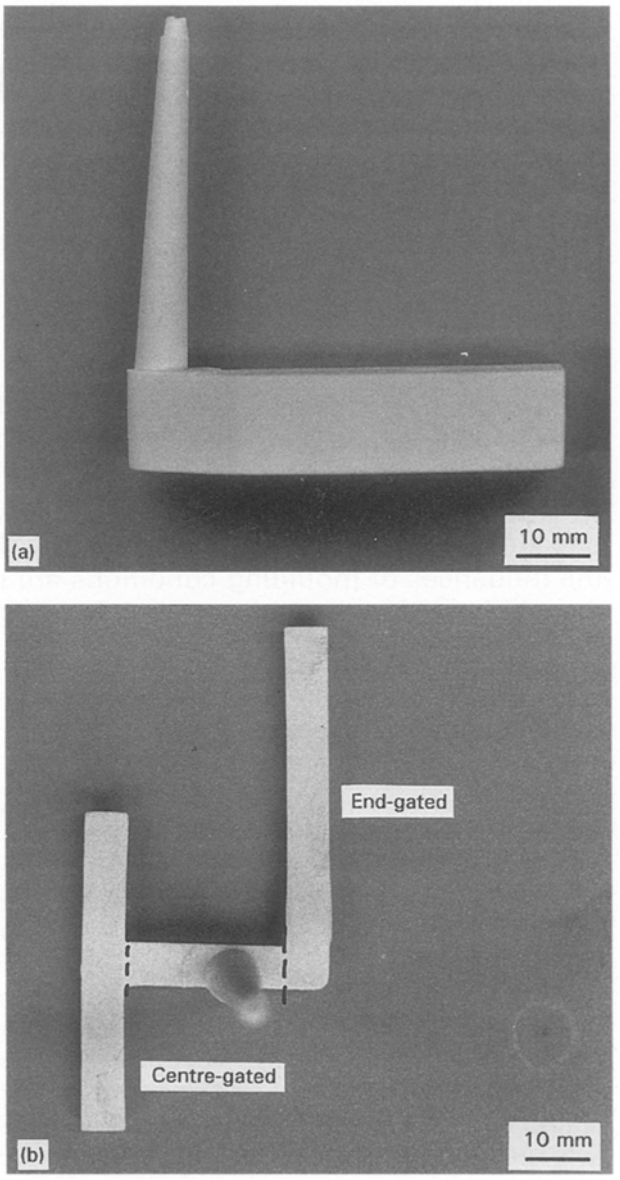

Figure 1 Injection-moulded samples: (a) thick section bars, type A, (b) end and side gate moulded bars, type B.

TABLE II Debinding conditions

Temperature range (°C)	Heating rate (°C h^{-1})	
	Full bars	Sections
20–110	10	10
110–300	2	5
300–450	15	15
450–900	60	60
900, for 1 h	0	0

Samples of type A and their sections, the annealed bars, and both type B samples were sintered for 1 h, at 1500 and 1650 °C for RA107LS and F1500 samples, respectively, with a heating rate of 1 °C min^{-1}. Densities of the sintered products were measured by the Archimedes' method after providing a thin cellulose varnish as coating.

The degree of bending, k, in the bars at any stage can be expressed by the curvature of the bent bar using the expression

$$k = 8y/l^2 \ (\mathrm{m}^{-1}) \quad (1)$$

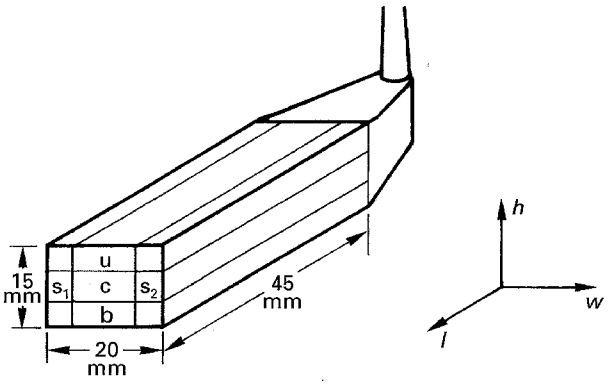

Figure 2 Positional relationships of cuts from thick section bars, Type A.

where y and l are the deformation and the length of the bar, respectively.

3. Results and discussion

3.1. Debinding and sintering defects

All bars made with F1500 powder with and without annealing were free from defects after debinding.

Bars made from RA107LS showed no visible defects in bars of type B. However, those of type A with the larger cross-section developed cracks during debinding, while the corresponding annealed bars were found to be free from cracks. This implies that crack development during debinding was related to a heterogeneous structure in the moulded components which was reduced with isostatic annealing. The observed heterogeneity may have arisen from: (1) binder separation or inhomogeneous mixing of the binder and powder, (2) residual stress, or (3) orientation of the binder and powder.

In order to distinguish between these effects, the densities of the sections of bars (Fig. 2) made with RA107LS powder and containing the binder were measured. The density measurements, the average of five samples for each position, are given in Table III. The difference in the densities was negligible, being less than 0.1% different from the paste density of 2917 kg m^{-3} calculated from the densities of the powder and the binders. This suggests that binder separation or mixing inhomogeneity was not significant in these materials.

The sections cut from the surface of the annealed bars and annealed again at 120 °C, were concave towards the surface due to the continued relaxation of the binder (Fig. 3a) [17]. This suggests that when highly loaded with fine particles the relaxation of the binder is only partly restricted in the bar. However, the relaxation was sufficient to reduce the thermal stresses and diminish the crack development during debinding of the full bars.

The bars which were free from external cracks after debinding were sintered and sectioned through the centre. All bars made with F1500 powder and bars of form B made with RA107LS powder were free from cracks throughout the body. However, bars of type A made with RA107LS powder showed extensive cracking both in the centre and at the surface. The

TABLE III The density distribution of green parts moulded from RA107LS at an injection pressure of 60 MPa. All the results are the average of five samples, with a standard error of less than 0.13%

Position	c	u	b	s_1	s_2
Density (kg m^{-3})	2914	2915	2918	2918	2918

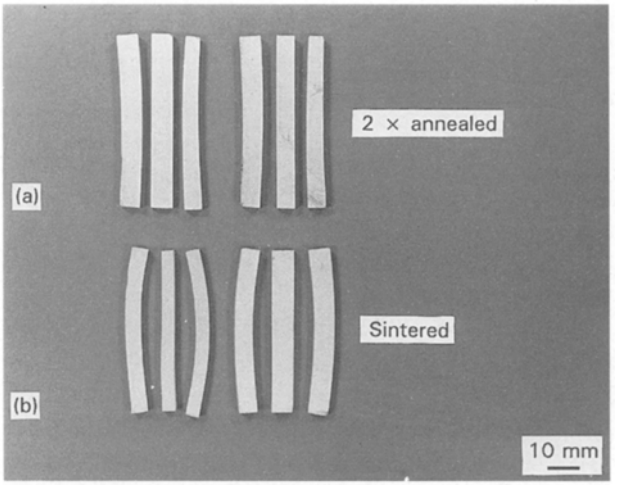

Figure 3 The bending of bars cut from large bars; left and right are top and bottom surfaces of the moulded bars, respectively (a) after annealing at 120 °C for 24 h. (b) after sintering.

cracks in two sintered samples, sectioned along the long axis, are shown in Fig. 4 and appear similar to the lamination cracks found in the interior of extruded objects [18]. When cut perpendicular to the bar axis they revealed differential shrinkage with the greatest shrinkage being in the centre. This shows the importance of a difference in shrinkage between the surface and centre in the moulded bars.

3.2. Different linear sintering shrinkage

The linear sintering shrinkage of sections cut from bars of type A made with RA107LS powder is shown in Table IV and it can be seen that it varied with position and direction within the bar. Three shrinkage directions were considered: length parallel to the long axis ($\Delta l/l_0$), height ($\Delta h/h_0$) and width ($\Delta w/w_0$) (Fig. 2). In the centre (c) $\Delta l/l_0$ was much larger than either perpendicular direction, $\Delta h/h_0$ or $\Delta w/w_0$. For samples cut from the surfaces (b and u), the largest shrinkage occurred with respect to height $\Delta h/h_0$ or $\Delta w/w_0$ depending on orientation, (b and u) or (s), respectively, these being the smaller shrinkages in the centre sections (c). Least variation in shrinkage was found with respect to $\Delta w/w_0$. Shrinkages of these materials under different moulding conditions are also shown in Table IV. It can be seen that the moulding condition had no significant effect on the shrinkages observed.

When sections were cut from bars of type A fabricated with F1500, the shrinkage in the three direction in all positions was taken to be uniform (Table IV), within the experimental error, quite different to the observations with RA107LS.

The end-gate moulded bars of type B made with RA107LS exhibited no visible defects after sintering. However, those moulded with a centre gate bent on sintering. No such defects were visible in bars fabricated from F1500.

The effect of moulding conditions on the shrinkage is small. However, the results indicate that the sintering shrinkage depends strongly on the particle properties, mould geometry and gate position. Anisotropic shrinkage promoted by these factors can increase sintering defects including both cracking and bending.

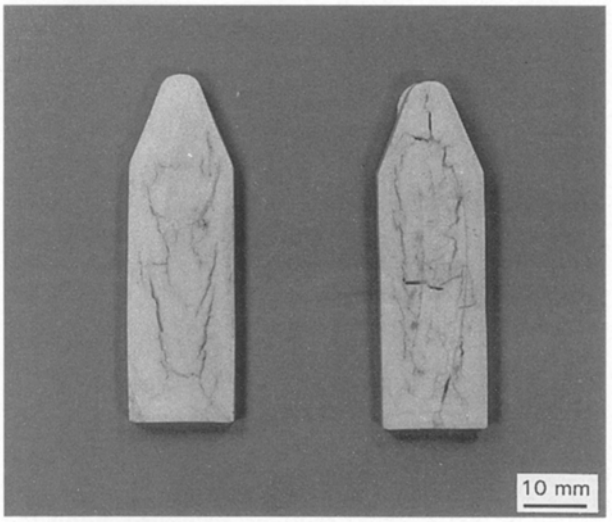

Figure 4 Sintering defects in RA107LS thick section bars after sintering, samples cut at the mid-line.

Complete bars of type A made with RA107LS powder were straight on sintering, because the non-uniform shrinkage properties were balanced within the bar. However, because the greatest shrinkage occurred in the centre of the bar, the outer surfaces tended to be drawn in, forming a concave lens-shaped body and the stresses due to the different shrinkages caused cracking within the sample.

When cut to form sections, the stress distribution of the off-centre samples was not symmetrical and thus, on sintering, curvature arose. In the long axis direction (l direction) the surface shrinkage was smaller than that in the centre and the sample bent, becoming concave with respect to the centre, Fig. 3b.

The bending of the sintered sections, k, is shown in Table IV. Possibly due to slight variations or asymmetry in sample cutting, the sections were not all exactly the same size, causing slight bending of the centre section and slight differences in the degree of curvature between top and bottom (u and b) sections and between the two side sections (s_1 and s_2).

3.3. Volumetric shrinkage

The volume shrinkage, $\Delta V/V_0$, of rectangular bars can be calculated from the linear shrinkages

$$\frac{\Delta V}{V_0} = 1 - \frac{(l_0 - \Delta l)(w_0 - \Delta w)(h_0 - \Delta h)}{l_0 w_0 h_0} \quad (2)$$

The volume shrinkages so calculated are included in Table IV. For all the sections, although the linear shrinkages were different, the volume shrinkages

TABLE IV The linear and volume shrinkages and curvature after sintering (mean of two samples)

Sample		Injection pressure (MPa)	Injection speed (% maximum available)	$\Delta l/l_0$ (%)	$\Delta w/w_0$ (%)	$\Delta h/h_0$ (%)	$\Delta V/V_0$ (%)	k (m^{-1})
RA107LS	c	60	20	15.0	11.2	11.8	33.9	2.5
	u			13.0	12.2	13.8	34.2	12.6
	b			12.2	11.0	14.6	33.3	4.6
	s_1			13.4	14.6	11.7	35.4	7.6
	s_2			12.9	15.9	12.1	35.5	7.5
RA107LS	c	40	20	15.6	12.1	11.1	34.2	3.0
	u			12.5	11.9	15.1	34.7	12.5
	b			12.6	11.5	15.2	34.4	5.6
	s_1			12.8	14.5	11.8	34.3	7.2
	s_2			13.1	14.2	11.7	34.2	9.1
RA107LS	c	20	20	15.3	12.4	11.6	35.3	3.8
	u			13.7	11.8	15.2	35.8	14.2
	b			12.6	11.5	15.4	34.5	5.2
	s_1			12.2	14.5	12.0	34.9	8.1
	s_2			13.3	14.3	11.9	35.3	8.4
RA107LS	c	20	5	15.3	12.4	11.7	34.4	3.1
	u			13.2	11.7	15.5	35.2	8.8
	b			12.4	11.5	15.5	34.6	2.8
	s_1			12.9	15.0	12.7	35.4	5.6
	s_2			13.8	14.8	11.9	35.2	7.1
F1500	c	60	20	13.8	13.8	13.5	36.4	0.0
	u			13.6	13.8	14.6	36.1	0.0
	b			13.6	14.0	14.2	35.8	0.8
	s_1			13.7	14.2	13.8	36.5	0.6
	s_2			14.0	13.6	12.9	35.1	0.0

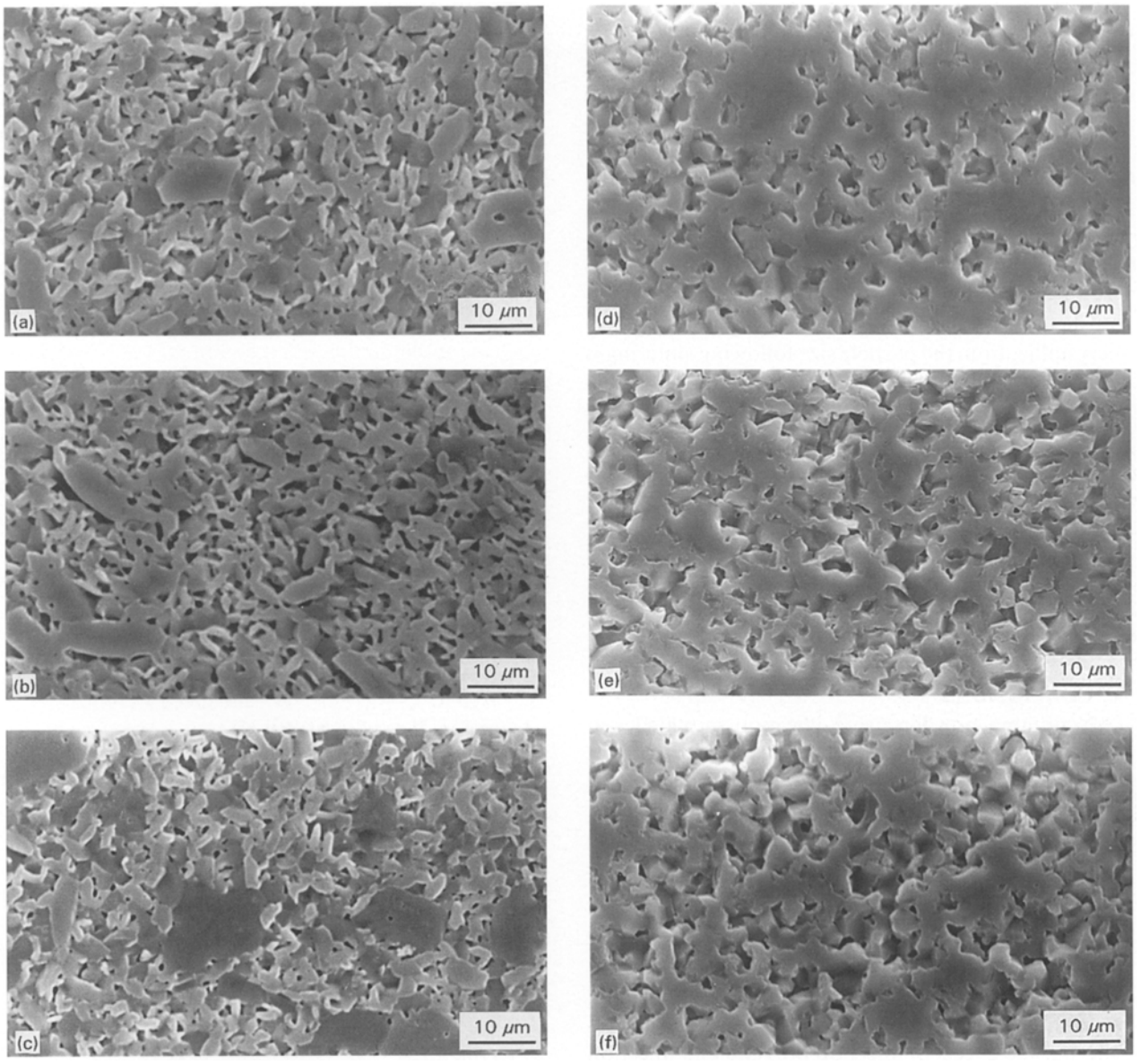

Figure 5 Microstructures of Type A RA107LS bars, (a) cut parallel to the flow direction, near the surface of the bar, and (b) near the centre, (c) cross-section, near the centre. Microstructure of F1500 bars (d) cut in the *l* direction, at the surface of the bar, and (e) near the centre, (f) cross-section, near the centre. The views are towards the external surface.

showed remarkably little variation. For the sections cut from the bars of type A made from RA107LS powder, the calculated volume shrinkage was near to the theoretical volume shrinkage of 35% for the fully dense parts. The measurements show, that all the sections have a relative density above 99% theoretical. However, owing to the temperature limitation of the furnace, the density of the sintered components made from F1500 powder only attained about 95% of the theoretical value.

If the linear shrinkages in three directions are equal, the linear shrinkage, $\Delta s/s_0$, can be found from the green density, d, and the density of the sintered body, d_s, because then

$$\frac{\Delta s}{s_0} = 1 - \left(\frac{d}{d_s}\right)^{1/3} \quad (3)$$

For RA107LS bars, the green density and the sintered density were 65% and 100% of the theoretical density, respectively. This corresponds to an isotropic linear shrinkage of 13.4%. For the centre section of the moulded body, the linear shrinkage in the axial direction, *l*, was greater than the calculated isotropic linear shrinkage. In the other two directions, the linear shrinkage was smaller than the isotropic shrinkage. For sections near to the mould surface, the linear shrinkages showed different trends. In particular, the linear shrinkage in the *h* direction was larger than the isotropic shrinkage. In sections of F1500 moulded samples, the green density and sintered density were 60% and 95% of the theoretical density, respectively, corresponding to an isotropic shrinkage of 14.2%. This is close to the measured shrinkages for all the sections, in all three dimensions. Anisotropic shrinkage will produce large stresses and may cause cracks to develop. Parts which have the same green density and sintered density, may have a different linear shrinkage. This is related to the powder properties and to the microstructure.

3.4. Particle orientation

Earlier work [17] has shown that when bars are moulded from plate-like powders, orientation occurs systematically. Near to the mould surface, the (0 0 1) plane of a RA107LS particle tends to lie parallel to the bar axis and the mould surface, whereas in the centre it lies perpendicular to the flow direction, despite the method of mould filling. This orientation can also be seen from the SEM studies of sintered RA107LS sections. Fig. 5 shows samples cut through the centre of the bar parallel to the l and w directions (Fig. 2), polished and etched with HF. Owing to secondary recrystallization, the particle size following sintering is larger than that of the green particles, but the microstructure shows that near the mould surface (Fig. 5a, 0.5 mm from the surface) the (0 0 1) plane tends to lie parallel to bar axis direction and the mould surface. Near the centre of the moulded component (Fig. 5b and c), the (0 0 1) plane lies perpendicular to the bar axis. No significant difference in the microstructure was observed in the F1500 samples, Fig. 5d (0.5 mm from the surface) and e and f (near the centre).

4. Conclusions

Two alumina powders were injection moulded and sintered in order to investigate the cause of defects during debinding and sintering. The sintering defects were observed by the viewing of fully sintered bars. The anisotropic linear shrinkages were assessed from sections cut at various locations in the samples. The results led to the following conclusions.

1. The anisotropic shrinkage during sintering is the main cause of defects in injection moulded parts.

2. The particle shape, mould geometry and gate position have a large effect on the shrinkage behaviour, but the effects of injection pressure and injection rate are small.

3. Plate-like particles become oriented during moulding. The plates tend to lie parallel to the moulding direction near the mould surface and change to be perpendicular to the moulding direction at the centre of the moulded bar. The linear shrinkage is smaller in a direction parallel to the plate than in a direction normal to the plates. Although the particle orientation causes anisotropic shrinkage, it does not affect the densification, at least for the parts of small cross-section studied here. However, anisotropy causes defects like bending or cracking due to internal stress development on sintering.

The closer that particles pack together in the unfired body in any particular direction, the smaller is the sintering shrinkage in that direction. If the particle spacing is uniform in all directions, the extent of filled space will differ if there is preferential orientation. In plate-like systems this results in differential shrinkage. For platelike particles it is thus necessary to take this into account when using injection moulding, especially of large cross-sections. Special consideration needs to be given to the processing and to developing understanding for paste systems with this class of particles.

Acknowledgement

The authors are grateful to the EPSRC for supplying funding of the Foundation Programmes of the IRC in Materials for High Performance Applications.

References

1. R. M. GERMAN, "Powder injection moulding" (Metal powder industries federation, Princeton, New Jersey, 1990, pp. 3–22.
2. B. C. MUTSUDDY, *Adv. Ceram. Mater.* **2** (1987) 213.
3. T. ZHANG and J. R. G. EVANS, *J. Am. Ceram. Soc.* **76** (1993) 481.
4. *Idem, J. Mater. Res.* **8** (1993) 345.
5. *Idem, Br. Ceram. Trans.* **92** (1993) 146.
6. M. R. BARONE and J. C. ULICNY, *J. Am. Ceram. Soc.* **73** (1990) 3323.
7. S. J. STEDMAN, J. R. G. EVANS and J. WOODTHORPE, *Ceram. Int.* **16** (1990) 107.
8. Y. BAO and J. R. G. EVANS, *J. Eur. Ceram. Soc.* **8** (1991) 81.
9. T. ZHANG and J. R. G. EVANS, *J. Mater. Sci. Lett.* **9** (1990) 672.
10. *Idem, J. Eur. Ceram. Soc.* **12** (1993) 51.
11. B. KOSTIC', T. ZHANG and J. R. G. EVANS, *J. Am. Ceram. Soc.* **75** (1992) 2773.
12. *Idem, Int. J. Powder Metall.* **29** (1993) 251.
13. P. ALLEN and M. BEVIS, *Plastics Rubber Process. Applic.* **3** (1983) 331.
14. R. W. COX and W. O. WILLIAMSON, *Trans. J. Brit. Ceram. Soc.* **57** (1958) 85.
15. H. WATANABE, T. KIMURA and T. YAMAGUCHI, *J. Am. Ceram. Soc.* **72** (1989) 289.
16. T. KIMURA, T. YOSHIMOTO, N. LIDA, Y. FUJITA and T. YAMAGUCHI, *ibid.* **72** (1989) 85.
17. T. ZHANG, S. BLACKBURN and J. BRIDGWATER, *J. Euro. Ceram. Soc.* in press.
18. G. C. ROBINSON in "Ceramic processing before sintering" edited by G. Y. Onoda, J. Larry L. Hench (Wiley, New York, 1978) pp. 391–401.

Received 16 February
and accepted 18 March 1996